

# Imaging the motion of the heart with echocardiography: advanced technology provides deeper insights into physiology and diastolic function

**S.J. Kovács**  
**L. Shmuylovich**  
**W. Zhang**

Cardiovascular Biophysics Laboratory, Cardiovascular Division,  
Washington University School of Medicine,  
St. Louis, MO, USA.

The pace of technological innovation in echocardiography remains impressive. For example, the Phillips iE33 provides novel live three-dimensional (Live 3D) imaging, and it also provides higher quality Doppler tissue and pulsed-wave Doppler imaging capabilities. With these new capabilities, clinicians can begin to image and quantitate, and thereby appreciate, subtle details related to diastolic physiology that with “old” technology may have been interpreted as “noise” and disregarded or averaged out. The application of these imaging capabilities in clinical practice presents both a challenge and an enormous opportunity in the field of cardiology.

## The meaning of “diastolic function”

Because of the acknowledged epidemic of heart failure [1-3], in particular diastolic heart failure [4-6], it has become increasingly important to understand the meaning of “diastolic function”. In clinical cardiology the term “diastolic function” is interpreted as relating to how the heart fills. By analogy the term “systolic function” is usually interpreted in terms of left ventricular ejection fraction (LVEF) where normal LVEF = (stroke volume)/(end-diastolic volume) falls in the 50% or greater range. No analogous simple, dimensionless parameter of diastolic function has been proposed. To appreciate the meaning of “diastolic function” the elegant and curious physiology of filling needs to be considered in some detail.

Common misconceptions remain about how the heart works when it fills. Diastolic function can be better understood when one appreciates that the left ventricle is a mechanical suction pump at, and for a little while after, mitral valve opening. In other words, at mitral valve opening, blood does not get pushed into the ventricle by the atrium, but is instead mechanically sucked in by the ventricle [7-9]. One may wonder where the energy driving suction arises, and the surprising answer is: systole. As the ventricle

contracts and overcomes the peripheral arterial load during ejection, it also compresses elastic elements both internal to and external to the myocardium. This stored elastic energy is released when enough of the cardiac muscle relaxes, and the elastic elements drive the recoil of the ventricle until a relaxed equilibrium configuration is achieved.

To fill effectively, a ventricle must remain compliant during filling (not be too stiff), quickly relax the “cramp” that was the previous systole (effective relaxation), and be able to physically accommodate the incoming blood volume. Thus stiffness and relaxation are intrinsic ventricular properties that are useful in determining and quantitating diastolic function, and volumetric load (also termed pre-load) represents the extrinsic parameter that modulates diastolic function.

## How to measure diastolic function

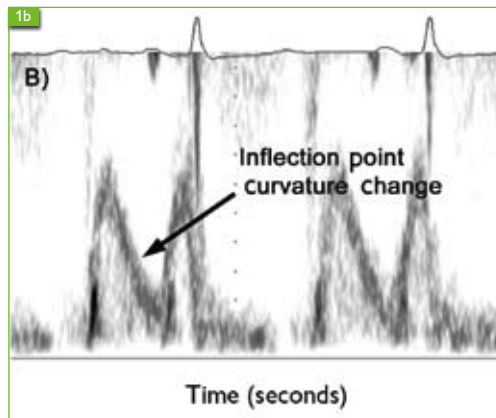
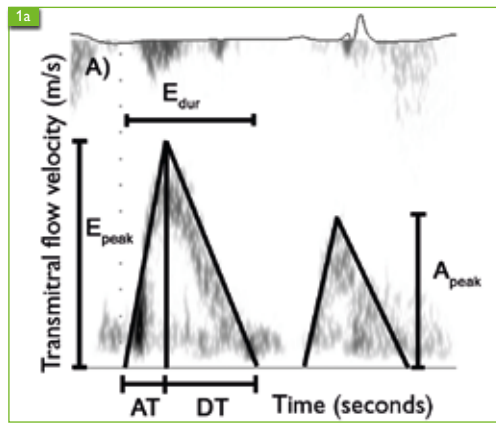
Many ideas have been tried with the intention of extracting both intrinsic and extrinsic ventricular properties. Early work focused on pulsed-wave Doppler-echo measured trans-mitral flow velocity contours. In terms of filling, diastolic intervals consist of early rapid filling E-waves followed by diastasis and followed by atrial systole-generated A-waves. As a first approximation, E- and A-wave contours were simplified as having triangular shape. To this day triangle-based indexes, including the peak heights of the E- and A-waves and their ratio,  $(E_{\text{peak}}, A_{\text{peak}}, E_{\text{peak}}/A_{\text{peak}})$ , the deceleration time and width (duration) of the E-wave ( $DT, E_{\text{dur}}$ ), and the velocity time integral (VTI) of the E- and A- waves (Figure 1A), are routinely measured. The use of a triangular approximation to the E-wave shape is convenient, especially when one considers the quality of images available using “old” technology. However, as a result of the improved temporal resolution and image processing capabilities of current technology, the curvature of E-wave contours

► **Innovation in echocardiography enables imaging of subtle details in diastolic function.**

► **Common misconceptions remain about how the heart works when it fills.**

Figure 1. The conventional triangle approximation to E- and A-wave shapes.

► Panel A). Conventionally, cardiologists have used the triangle approximation to characterize E- and A-waves. Using this approximation, the peak heights of the E- and A-waves ( $E_{peak}$ ,  $A_{peak}$ ), the duration of the E-wave ( $E_{dur}$ ), acceleration time (AT), deceleration time (DT), ratio of peak heights ( $E_{peak}/A_{peak}$ ), ratio of velocity time integrals ( $E_{VTI}/A_{VTI}$ ) are measured.



► Panel B). An example of the curvature change (inflection point) of the E-wave contour.

can clearly be discerned and the information they convey can be determined (Figure 1B). Despite these advances, physiologically important curvature features of the E-wave are usually disregarded. However, there is benefit in understanding the physical and physiological principles that govern the curvature, and this is discussed in more detail below (parametrized diastolic filling [PDF] model).

Technological advances allow the measurement of even smaller (i.e. tissue) velocities. This allows measurement of the longitudinal displacements of the mitral annulus. Once again, the shapes of mitral annular velocity contours were initially considered as triangles, with determination only of the peak, labeled E'. E' proved useful in selected patient populations for estimation of end-diastolic pressure (EDP) [8]. Improved technology has revealed further details regarding the curvature and oscillations of the E'-wave and these detailed insights are discussed at greater length below.

Additional novel imaging capabilities include techniques such as speckle tracking, which allows for strain and strain-rate measurements. Speckle tracking is a recent example of technological progress, because it relies on the information content inherent in the seemingly random arrangement of bright speckles present in all echocardiographic images [10].

While the various echo-based imaging modalities represent different levels of technological innovation, much remains to be learned in relation to how to interpret the recorded data. In the kinematics-based approach utilized here, the use of physical models and mathematical techniques is advocated in order to extract relevant information from all modes of imaging and thereby more fully understand the rules that govern how the heart works when it fills.

## Pulsed-wave Doppler imaging

### The parametrized diastolic filling (PDF) formalism

In routine practice, the curvature of the E-wave is ignored when the E-wave is approximated as a triangle. By considering the kinematic analog of the role of the heart as a suction pump, a deeper understanding into the physiological determinants of E-wave curvature has been gained, thereby making the triangular approximation unnecessary.

The filling of the ventricle can be modeled by comparing it to a recoiling spring (a mechanical oscillator) that has an inertial load and is moving against a resistance [11]. The model is called the parametrized diastolic filling (PDF) formalism. To be specific, this formalism (kinematic model) stems from Newton's Laws of Motion and characterizes the E-wave in terms of a driving force (the atrio-ventricular pressure gradient), a damping/viscous force that resists trans-mitral flow, and an inertial load due to tissue and blood.

Using this model, by solving the associated differential equation, mitral flow velocity can be mathematically predicted as the solution to the equation of motion. In other words: all ventricles are mechanical suction pumps, and fill by obeying the same law of motion. The parameters that specify the motion, however, vary from heart to heart. As a simple analogy consider the trajectory of a stone thrown in the air. The arc the stone makes varies from throw to throw, and depends on the initial velocity and angle of launch, while the laws of inertia and gravity that determine the stone's trajectory remain the same for each throw.

Each mitral flow E-wave can be uniquely determined by three parameters: the initial displacement of the spring  $x_0$ , which is linearly related to the E-wave VTI (i.e. volumetric preload) [8], a stiffness parameter  $k$ , which is linearly related to chamber stiffness ( $dP/dV$ ) [12] and a resistance/damping parameter or chamber viscoelasticity/relaxation index  $c$  (g/s)

► **The PDF formalism considers the ventricles of the heart to be mechanical suction pumps.**

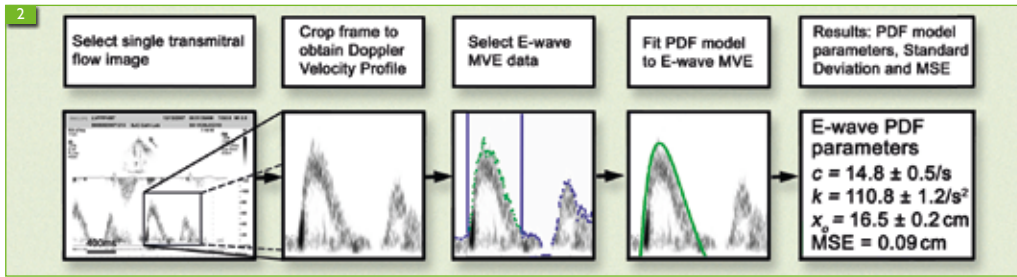


Figure 2. Quantitation of diastolic function via model-based image processing (MBIP) using the parametrized diastolic filling (PDF) formalism. After the E-wave is cropped, the maximum velocity envelope (MVE) is identified and is fitted numerically by the solution to the PDF model, yielding the three, unique, best-fit PDF parameters ( $x_0$ ,  $c$ ,  $k$ ) and a measure of goodness-of-fit.

which accounts for filling-related energy losses [8]. The spring constant,  $k$ , primarily determines the width of the E-wave. A high spring constant (i.e. a stiff spring) will generate a tall narrow E-wave as seen in the “constrictive-restrictive” pattern. The resistance/damping parameter is mainly responsible for the tail of the E-wave and is directly responsible for the inflection point (change in curvature from “cup-down” to “cup-up”) seen in the deceleration portion. A high value for the resistance/damping parameter in general gives rise to the “delayed relaxation” pattern on the E-wave. Accordingly, the resistance/damping parameter,  $c$ , can be used as a relaxation parameter.

The PDF model parameters ( $x_0$ ,  $c$ ,  $k$ ) for each E-wave can be obtained through model-based image processing (MBIP), detailed in Figure 2. Shortly after the E-wave is selected, the maximum velocity envelope is identified and is fitted numerically by the solution to the PDF equation, yielding the three best-fit PDF parameters ( $x_0$ ,  $c$ ,  $k$ ) and a measure of goodness-of-fit.

With a mathematically accurate model of the E-wave, subtle details of curvature that are

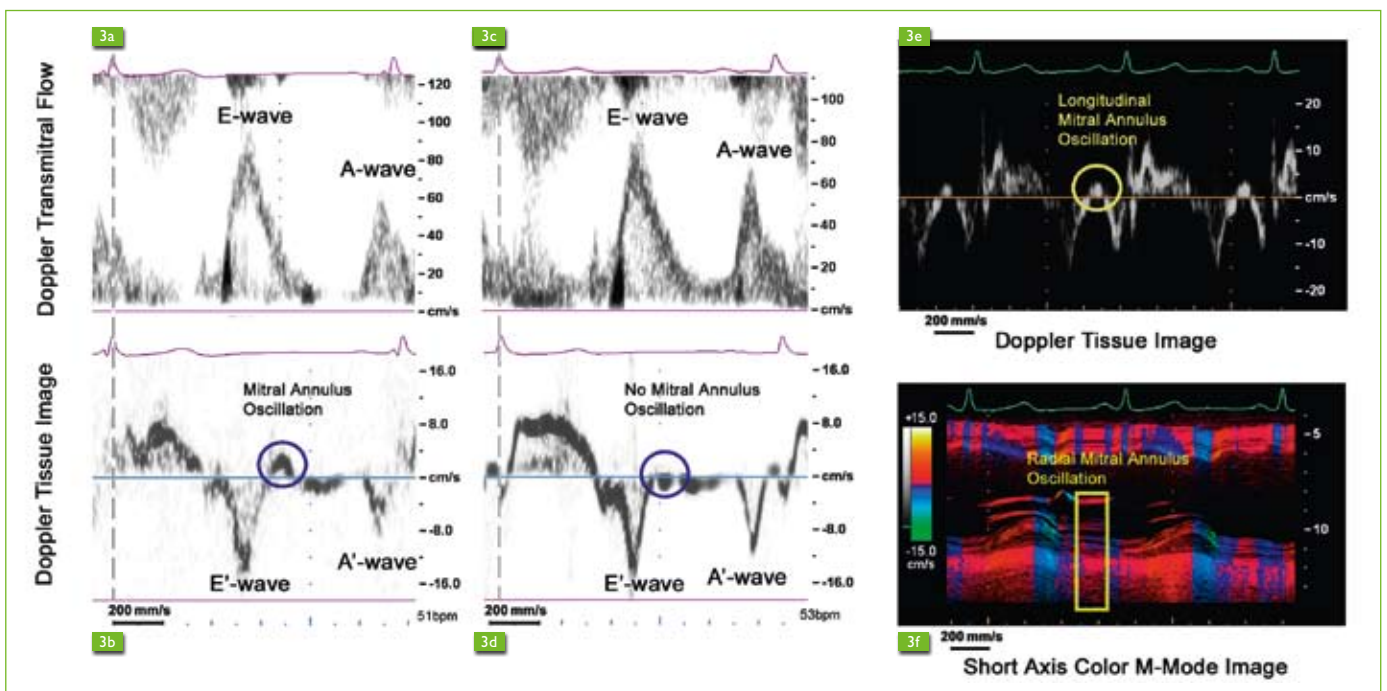
absent in the triangular shape approach, prove to be useful. The analysis of E-waves via this model has shown that diabetes increases the resistance/relaxation parameter,  $c$ , of early rapid filling in both rats [13] and humans [14]. Importantly, these two studies showed that for hearts with normal LVEF, in contrast to the relaxation/viscosity parameter,  $c$ , conventional E-wave indexes, such as  $E_{peak}$  or DT, were unable to differentiate between normal and diabetic subjects. A further manifestation of the resistance/relaxation property of the ventricle is that all ventricles fill to a volume that is less than the maximum (lossless) ideal filling volume. An index which characterizes this efficiency of filling, the kinematic filling efficiency index (KFEI) has been shown to be lower in normal LVEF diabetics compared to normal controls [15]. Furthermore, the resistance/relaxation parameter,  $c$ , has been shown to be linearly related to relaxation characterized by  $\tau$ , the (invasively-determined) time constant of isovolumic relaxation [16].

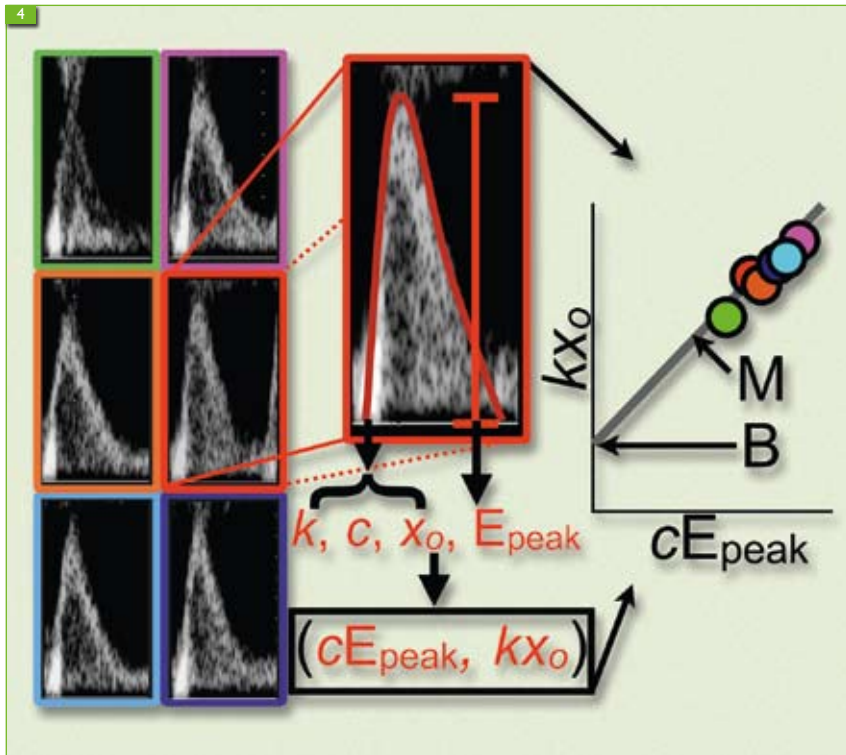
### Doppler tissue imaging (DTI)

Doppler tissue imaging (DTI) has become routine in diastolic function assessment.

Figure 3. Echocardiographic presence of longitudinal (mitral annulus oscillation [MAO]) and radial oscillation.

- Trans-mitral flow.
- Contemporaneous Doppler tissue imaging (DTI) of lateral aspect of mitral annulus indicating longitudinal MAO.
- Trans-mitral flow of a different subject.
- Contemporaneous DTI of lateral aspect of mitral annulus of the same subject, with absence of longitudinal MAO.
- Longitudinal MAO in another subject.
- Contemporaneous color m-mode Doppler short axis image showing radial oscillation. Images are synchronized using an electrocardiogram (ECG).





▲ Figure 4. How the load-independent index of diastolic function (LIIDF) is determined for a set of varying E-waves. LIIDF determination requires multiple E-waves with different shapes. In this case six waves were employed, though depending on the circumstance more waves may be necessary. In the center the analysis of one E-wave is highlighted (red frame border). Using model-based image processing (MBIP) a parametrized diastolic filling (PDF) model fit is generated (red E-wave contour) and the parameters  $k$ ,  $c$  and  $x_0$  are determined, as described in Figure 1. The height of the wave ( $E_{peak}$ ) is measured. The quantities  $(c)(E_{peak})$  and  $(k)(x_0)$  are computed, the point  $(cE_{peak}, kx_0)$  for that single E-wave is plotted in the  $kx_0$  vs.  $cE_{peak}$  plane. (red dot on graph). Each wave (denoted by a color) determines one point in the  $kx_0$  vs.  $cE_{peak}$  plane. Each wave is color coded with its corresponding point for clarity. The linear regression determined by the points in the  $kx_0$  vs.  $cE_{peak}$  plane defines a slope  $M$  and intercept  $B$ . The slope  $M$  is the dimensionless LIIDF.

However, with past technology it was difficult to appreciate the shape of the DTI generated E'-wave and subsequent multiple annular oscillations, which has been previously noted [17-19]. Such oscillations may have been considered to be noise. Importantly, these annular oscillations obey the laws of oscillatory motion and thereby are amenable to MBIP-based quantitation [20-22]. With current technology, the presence or absence of oscillations is clearly evident, as shown in Figure 3.

The ability to image longitudinal and radial motion to high precision has permitted characterization of spatially distinct compensatory mechanisms in diastole. In other words, because maintenance of cardiac output and stroke volume constitute the prime directives in survival, it follows that impairment of longitudinal motion should be accompanied by compensation in radial motion in order to preserve stroke volume.

The information obtained from DTI holds great potential for diagnosis of diastolic relaxation abnormalities. The absence of mitral annulus oscillation (MAO) is a good predictor of relaxation-related diastolic dysfunction. In a recent study, it was found that patient groups without MAO tended to have prolonged  $\tau$  and isovolumic relaxation time (IVRT), lower  $E_{peak}/A_{peak}$  and E'-waves, and increased  $E_{peak}/E'$  [23]. With advancing technology, cardiologists can easily and reliably utilize MAO to gain additional information about diastolic function.

## Characterization of the effects of weight loss on diastolic function and aging of the heart

The PDF formalism has been used in the investigation of the effects of caloric restriction and exercise-induced weight loss on diastolic function. It has been found that both caloric restriction and exercise-induced weight losses have beneficial effects on diastolic function [24]. In addition the PDF parameters of subjects with caloric restriction were more in line with PDF parameters observed in a younger cohort, implying that caloric restriction slows "aging" in the normal heart [25].

## Load-independent index of diastolic function (LIIDF)

A constant challenge in clinical quantitation of diastolic function relates to measuring diastolic function using data that is confounded by a patient's load state. As discussed above, diastolic function can be characterized in terms of intrinsic parameters (stiffness and relaxation) and extrinsic parameters (load state). In clinical echocardiography, despite advancing imaging capabilities, traditional ( $E_{peak}/A_{peak}$ , VTI, acceleration time [AT], DT) and newer echo-derived indices ( $E/E'$ , strain, strain rate, Velocity of propagation (Vp), etc.) have all been documented to be load-dependent. Thus, it is not currently possible to echocardiographically determine diastolic function in terms of load-independent measures of chamber stiffness and relaxation. In other words, a load-independent index of diastolic function (LIIDF), though clinically desired, is not currently available on any echocardiographic platform.

The situation is analogous to determining the quality of brakes by measuring the braking distance of a car. One car may take 50 feet to stop on a dry road, while another requires 80 feet to stop on a wet road. In this situation the road-independent, intrinsic braking function cannot be determined. In the clinical realm, quantitation of diastolic function is indeed blind to the "road". In fact, in the clinical setting, load-dependence of echo-indexes can lead conventional echocardiographic indexes (such as  $E_{peak}/A_{peak}$ ) in healthy subjects to appear abnormal, or in subjects with pathophysiology ( $E_{peak}/A_{peak} < 1$ ) to pseudonormalize.

With no reliable LIIDF available, clinical practice has focused instead on averaging measurements from multiple beats. For example, in analyzing the  $E_{peak}$ , one would measure several consecutive E-waves, and then report the average  $E_{peak}$ . Thus, if any information regarding diastolic function is present in the actual beat-to-beat variation, then this information is lost due to averaging.

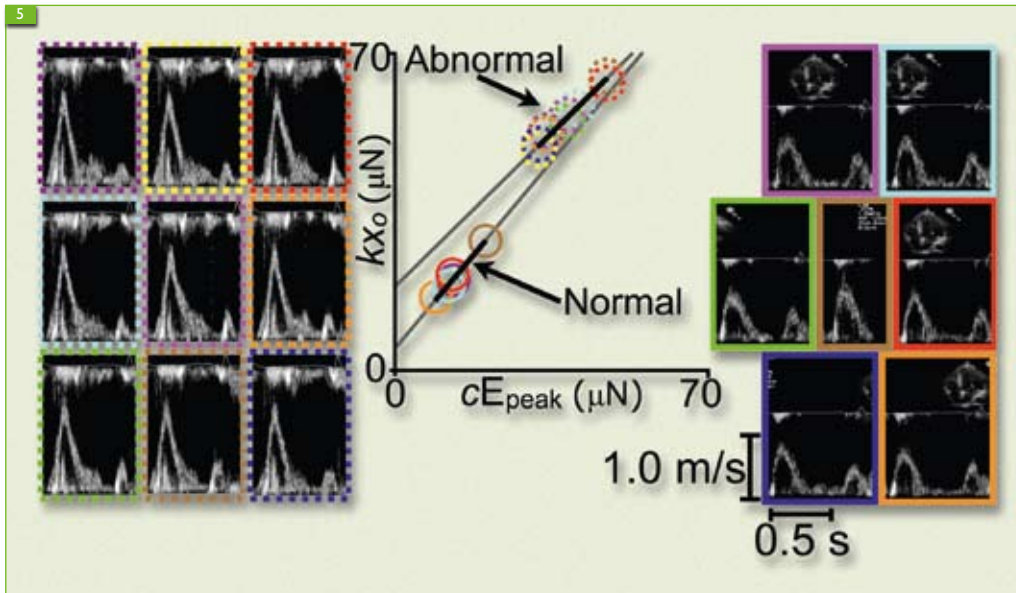


Figure 5. Contrasting normal vs. abnormal diastolic function in terms of the load-independent index of diastolic function (LIIDF).

Left panel: Nine trans-mitral flow images from a subject with an end-diastolic pressure (EDP) of 35 mmHg (abnormal diastolic function).

Right panel: Seven trans-mitral flow images from a subject with an EDP of 12 mmHg (normal diastolic function).

For each E-wave a corresponding  $cE_{\text{peak}}$  and  $kx_0$  value was determined and plotted on the  $kx_0$  vs.  $cE_{\text{peak}}$  plot. Thus nine E-waves with dotted frame borders define nine points, shown as dotted circles. Similarly seven E-waves with solid frame borders define seven points, shown as solid circles. The  $kx_0$  vs.  $cE_{\text{peak}}$  regression for nine dotted points is  $M = 0.95$ ,  $B = 19.0$ ,  $r^2 = 0.98$ , the regression for the seven solid points is  $M = 1.15$ ,  $B = 5.10$ ,  $r^2 = 0.99$ . Notice both regressions are highly linear, but the subject with abnormal diastolic function has a lower slope ( $M$ ) and higher intercept ( $B$ ) compared to the normal subject.

In a recent study, a solution to the LIIDF problem was found. Mathematical analysis of E-wave shapes reveals a novel index that is extremely well conserved in the face of load variation [26]. The key insight into extracting this load-independent index lies in analyzing not just one, but several E-waves, all preferably acquired at varying load states (Figure 4). To determine the LIIDF, first stiffness ( $k$ ), damping ( $c$ ) and initial stretch parameters ( $x_0$ ) for each E-wave, as described above, were extracted. In addition, the peak height of the E-wave ( $E_{\text{peak}}$ ) was measured. For each E-wave, the product of  $k$  and  $x_0$  gives us the model-predicted maximum driving force promoting forward flow, which is the analog of the peak instantaneous atrio-ventricular pressure gradient. The product of each E-wave's  $c$  and  $E_{\text{peak}}$  defines the maximum resistive force opposing atrio-ventricular flow. Thus, for each E-wave a  $kx_0$  value and the associated  $cE_{\text{peak}}$  value was computed, and as a result each E-wave represents a point in the  $kx_0$  vs.  $cE_{\text{peak}}$  graph. The LIIDF is the slope,  $M$ , of the linear regression between all ( $cE_{\text{peak}}$ ,  $kx_0$ ) points, where each point is extracted from a separate E-wave.

The initial work studied healthy volunteers subjected to tilt-table maneuvers to change load, and cardiac catheterization patients with load variation due to respiration. Healthy subjects showed significant E-wave shape changes as the tilt angle was varied from upright to supine to head-down. Despite the dramatic visual E-wave shape variation, all associated ( $cE_{\text{peak}}$ ,  $kx_0$ ) points remained co-linear ( $R^2 = 0.98$ ), demonstrating that the slope of the  $kx_0$  vs.  $cE_{\text{peak}}$  regression is a constraint on E-wave shape that is independent

of load. Furthermore, it was found that in subjects undergoing cardiac catheterization the LIIDF slope ( $M$ ) was significantly lower in subjects having diastolic dysfunction (elevated filling pressures  $> 18$  mmHg), compared to subjects with normal diastolic function (Figure 5). Thus, the LIIDF is easily determined by analysis of a series of load-varying E-waves, is constant in the face of load variation and differentiates between normal diastolic subjects and subjects with diastolic dysfunction. The method of LIIDF determination relies critically on the differences between E-wave shapes. The practical utility and clinical power of the LIIDF resides in its application in sequential studies, where each subject serves as their own control. Using this approach, whether therapy has resulted in “beneficial” or “adverse remodeling”, LIIDF can be assessed in load-independent terms. Furthermore the LIIDF in and of itself can serve as a therapeutic target for diastolic function improvement.

## Future applications

The future is bright because improvements in imaging speed, fidelity and processing will continue to emerge. In principle this will allow a more complete “model-based image analysis” approach to quantitatively characterize fluid and heart tissue motion. The PDF approach, and the LIIDF developed from it, are early harbingers of things to come, ultimately leading to automated, observer-independent, quantitative assessment of four-chamber heart function at the push of a button. Of course the important role of the sonographer will remain, but technology will do more than its share to advance the science and art of diagnosis and assessment of therapy ■

► The future may lead to automated assessment of heart function at the push of a button.

## References

- [1] Bleumink GS, Knetsch AM, Sturkenboom MCJM, Straus SMJM, Hofman A, Deckers JW, et al. *Quantifying the Heart Failure Epidemic: Prevalence, Incidence Rate, Lifetime Risk and Prognosis of Heart Failure: The Rotterdam Study*. Eur Heart J. 2004; 25(18): 1614-1619.
- [2] Redfield MM. *Heart Failure - An Epidemic of Uncertain Proportions*. N Engl J Med. 2002; 347(18): 1442-1444.
- [3] Schocken DD, Arrieta MI, Leaverton PE, Ross EA. *Prevalence and Mortality Rate of Congestive Heart Failure in the United States*. J Am Coll Cardiol. 1992; 20(2): 301-306.
- [4] Bhatia RS, Tu JV, Lee DS, Austin PC, Fang J, Haouzi A, et al. *Outcome of Heart Failure with Preserved Ejection Fraction in a Population-Based Study*. N Engl J Med. 2006; 355(3): 260-269.
- [5] Owan TE, Hodge DO, Herges RM, Jacobsen SJ, Roger VL, Redfield MM. *Trends in Prevalence and Outcome of Heart Failure with Preserved Ejection Fraction*. N Engl J Med. 2006; 355(3): 251-259.
- [6] Redfield MM. *Understanding "Diastolic" Heart Failure*. N Engl J Med. 2004; 350(19): 1930-1931.
- [7] Katz LN. *The Role Played by The Ventricular Relaxation Process in Filling The Ventricle*. Am J Physiol. 1930; 95(3): 542-553.
- [8] Kovács SJ, Meisner JS, Yellin EL. *Modeling of Diastole*. Cardiol Clin. 2000; 18(3): 459-487.
- [9] Robinson TF, Factor SM, Sonnenblick EH. *The Heart as a Suction Pump*. Sci Am. 1986; 254(6): 84-91.
- [10] Helle-Valle T, Crosby J, Edvardsen T, Lyseggen E, Amundsen BH, Smith HJ et al. *New Noninvasive Method for Assessment of Left Ventricular Rotation: Speckle Tracking Echocardiography*. Circulation. 2005; 112(20): 3149-3156.
- [11] Kovács SJ Jr, Barzilai B, Pérez JE. *Evaluation of Diastolic Function with Doppler Echocardiography: The PDF Formalism*. Am J Physiol. 1987; 252(1 Pt 2): H178-187.
- [12] Kovács SJ, Setser R., Hall AF. *Left Ventricular Chamber Stiffness from Model-Based Image Processing of Transmitral Doppler E-Waves*. Coron Artery Dis. 1997; 8(3-4): 179-187.
- [13] Dent CL, Bowman AW, Scott MJ, Allen JS, Lisauskas JB, Janif M et al. *Echocardiographic Characterization of Fundamental Mechanisms of Abnormal Diastolic Filling in Diabetic Rats with a Parameterized Diastolic Filling Formalism*. J Am Soc Echocardiogr. 2001; 14(12): 1166-1172.
- [14] Riordan MM, Chung CS, Kovács SJ. *Diabetes and Diastolic Function: Stiffness and Relaxation from Transmitral Flow*. Ultrasound Med Biol. 2005; 31(12): 1589-1596.
- [15] Zhang W, Chung CS, Riordan MM, Wu Y, Shmuylovich L, Kovács SJ. *The Kinematic Filling Efficiency Index of the Left Ventricle: Contrasting Normal vs. Diabetic Physiology*. Ultrasound Med Biol. 2007; 33(6): 842-850.
- [16] Chung CS, Ajo DM, Kovács SJ. *Isovolumic Pressure-to-Early Rapid Filling Decay Rate Relation: Model-Based Derivation and Validation via Simultaneous Catheterization Echocardiography*. J Appl Physiol. 2006; 100(2): 528-534.
- [17] Isaaz K, Munoz del Romeral LM, Lee E, Schiller NB. *Quantitation of the Motion of the Cardiac Base in Normal Subjects by Doppler Echocardiography*. J Am Soc Echocardiogr. 1993; 6(2): 166-176.
- [18] Wiggers CJ. *Dynamics of Ventricular Contraction under Abnormal Conditions*. Circulation. 1952; 5(3): 321-348.
- [19] Zaky A, Grabhorn L, Feigenbaum H. *Movement of the Mitral Ring: A Study in Ultrasoundcardiography*. Cardiovasc Res. 1967; 1(2): 121-131.
- [20] Riordan MM, Kovács SJ. *Elucidation of Spatially Distinct Compensatory Mechanisms in Diastole: Radial Compensation for Impaired Longitudinal Filling in Left Ventricular Hypertrophy*. J Appl Physiol. 2008; 104(2): 513-520.
- [21] Riordan MM, Kovács SJ. *Quantitation of Mitral Annular Oscillations and Longitudinal "Ringing" of the Left Ventricle: A New Window into Longitudinal Diastolic Function*. J Appl Physiol. 2006; 100(1): 112-119.
- [22] Riordan MM, Kovács SJ. *Stiffness- and Relaxation-Based Quantitation of Radial Left Ventricular Oscillations: Elucidation of Regional Diastolic Function Mechanisms*. J Appl Physiol. 2007; 102(5): 1862-1870.
- [23] Riordan MM, Kovács SJ. *Absence of Diastolic Mitral Annular Oscillations is a Marker for Relaxation-Related Diastolic Dysfunction*. Am J Physiol Heart Circ Physiol. 2007; 292(6): H2952-2958.
- [24] Riordan MM, Weiss EP, Meyer TE, Ehsani AA, Racette SB, Villareal DT et al. *The Effects of Caloric Restriction- and Exercise-Induced Weight Loss on Left Ventricular Diastolic Function*. Am J Physiol Heart Circ Physiol. 2008; 294(3): H1174-1182.
- [25] Meyer TE, Kovács SJ, Ehsani AA, Klein S, Holloszy JO, Fontana L. *Long-Term Caloric Restriction Slows Cardiac Aging in Humans*. J Am Coll Cardiol. 2006; 47(2): 398-402.
- [26] Shmuylovich L, Kovács SJ. *Load-Independent Index of Diastolic Filling: Model-Based Derivation with In Vivo Validation in Control and Diastolic Dysfunction Subjects*. J Appl Physiol. 2006; 101(1): 92-101.